REVEALING CELTIC FIELDS FROM LIDAR DATA USING KRIGING BASED FILTERING

Astrid Humme[1], Roderik Lindenbergh[1] and Chris Sueur[2]

1: Delft University of Technology, Delft Institute of Earth Observation and Space Systems;
A.J.M.Humme@student.TUDelft.NL, R.C.Lindenbergh@lr.tudelft.nl
2: Vestigia B.V.; c.sueur@vestigia.nl

KEY WORDS: LIDAR, archaeology, filtering, geostatistics

ABSTRACT:

A detailed elevation model of the Netherlands has been acquired with the use of Airborne Laser Altimetry and is managed by AHN (Actueel Hoogtebestand Nederland). This elevation model can be used for a large amount of applications. Using a suited illumination technique it turned out to be possible to find and visualize so-called Celtic fields, agricultural fields systems of about 2500 years old in the AHN data. Here we will show that the visualization of Celtic fields out of AHN data can be enhanced by applying a geostatistical filter technique that removes the raw topography from the data set such that only the micro-topography, including the Celtic fields, remains. Visualization of this micro-topography not only enhances the images of the already known Celtic fields but also shows that the spatial extend of the field system is larger than expected.

1. INTRODUCTION

Celtic fields are prehistoric agricultural field systems that are recognizable as rectangular patches of land of about 40 $\times$ 40 meter surrounded by low earth walls, see Fig. 1. The highlight of the use of Celtic fields was between 800 B.C. and 0 B.C. and they can be found in several countries in North-West Europe, (Spek, Groenman-van Waateringe, Kooistra, and Bakker, 2003). In open land Celtic field systems are often still recognizable, even from the ground, although it is easier to distinguish them by color changes in areal photo's. Unfortunately it is very difficult to find Celtic field systems in forest areas, as small elevation differences or small color changes are completely masked by the forest cover.

Figure 1. Impression of a Celtic field system. (Rob Beentjes)

It turns out however that, even in forest areas, Celtic field systems can be found by analyzing airborne laser altimetry data, (Zijverden and Laan, 2005). Several approaches exist to obtain the bare earth surface out of raw airborne laser scanning point clouds, (Sithole and Vosselman, 2004). After removing points that were reflected by trees or shrubs, the remaining points are assumed to represent the ground surface. In this way it is possible to look for archeological features under the trees, (Da Devereux, Amabable, Crow, and Cliff, 2005).

In The Netherlands, the Dutch Ministry of Public Works initiated the setup of the so-called Actueel Hoogtebestand Nederland (AHN), that can be translated as 'Up to date height data base of The Netherlands'. This database consists of interpolated airborne laser altimetry data covering the whole of The Netherlands, containing at least one point per 4 m^2 outside and one point per 16 m^2 inside forest areas, (Anonymous, 2000). The accuracy of the laser altimetry technique depends strongly on the amount of vegetation and topography in the area. AHN states that for the accuracy of solid topography (such as roads and parking lots) as well as flat or soft topography (such as beaches and grass-fields) a standard deviation of 15 cm maximum applies, with a systematical error of 5 cm maximum.

Figure 2. Celtic fields, inside the circle, revealed by illumination.

This elevation model can be used for a large amount of applications, including many archeological, see also (De Boer, Laan, Waldus, and Van Zijverden, ToAp). The third author of this paper applied a technique based on illumination to visualize ancient Celtic fields, near Doorwerth, situated in the East of the Netherlands, out of AHN data. Figure 2 shows the fields as exposed by the third author. By illuminating the ground surface points in a suited way in a software visualization program, some unknown field systems could be traced by the shadows of the micro-relief of the low earth walls.

In our contribution we show that this approach can be still improved. In the original approach, the micro-relief is visualized with respect to the natural relief of the ground surface as it is represented in the laser data. By filtering the large scale topography the micro-relief becomes more prominent: only small-scale features like road beds, foot-paths and the earth walls surrounding

the Celtic fields remain. The height difference of about 70 meter in the original data is reduced to about 50 centimeter in the micro-relief data that remains from the original data after filtering away the coarse topography.

The filtering is done by means of the geostatistical Kriging method, (Goovaerts, 1997; Wackernagel, 2003), a special case of BLUP, Best Linear Unbiased Prediction, (Teunissen, 2000). In this method information on correlation between observations and relative quality of individual observations is used to attach weights to observations for a prediction at a certain location, e.g. near a Celtic field. If a long correlation distance is used, more weight is attached to more far observations, which will result in a smooth representation of the ground surface. Subtracting the smoothed data from the original data results in the micro-relief data that are used as input for the Celtic fields visualization.

This paper is organized as follows. In Section 2. it is explained how the method of factorial Kriging can be used to separate data components of different scale. In Section 3. the used parameter values and the final results of the separation algorithm are presented, followed by discussion of the results in Section 3.

2. FILTERING METHODOLOGY

In this section we describe a geostatistical 2D filter method for separating the coarse topography from the micro-scale relief. Geostatistics, see (Goovaerts, 1997), is a class of probabilistic interpolation methods, generally known as Kriging, that considers observations as outcomes of a random process. The Kriging method is a subset of a much larger family of linear estimation and prediction methods that incorporates the variations in observations and correlation between observations in variance-covariance matrices, (Teunissen, 2000; Koch, 1999). Kriging is just one way to separate spatial components of different scale. The method described here is sometimes referred to as Factorial Kriging, see (Goovaerts, 1997; Chilès and Delfiner, 1999). Elsewhere, (Lindenbergh, van Dijk, and Egberts, ToAp), the results of Kriging based filtering and separation of spatial components by means of Fourier theory are compared in separating morphological seafloor bed-forms as sampled by Multi-beam Echo sounding data.

In the following it is first described how to encode the spatial continuity of the large scale topography in a covariance function. This covariance function is used to fill the redundancy matrix and the proximity vector that contain the inter-observation correlations and the correlations between the observation locations and the location of prediction. This first exploratory step is generally referred to as the structural analysis of the observations. The redundancy matrix and the proximity vector are the main constituents of the Kriging system that is solved for every observation location to obtain a prediction for the large scale topography component. Subtracting these large scale predictions from the original observations will give us finally the micro-relief that is aimed for.

2.1 Structural Analysis

Throughout this section $Z_1, \ldots, Z_n$ denote n AHN height observations at horizontal observation locations $\mathbf{p}_1, \ldots, \mathbf{p}_n$. The spatial variability of a stationary signal $Z(.)$ can be determined by constructing an experimental covariance function. The stationarity condition assumes that the covariance

$$\text{cov}(\mathbf{h}) \;=\; E\{(Z(\mathbf{p}) - \mu)(Z(\mathbf{p}+\mathbf{h}) - \mu)\} \tag{1}$$

is independent of the location, $\mathbf{p}$, and therefore only depends on the difference in location $\mathbf{h}$. Here, μ denotes the mean $\mu = E\{Z(\mathbf{p})\}$. By computing all pair-wise experimental covariances

$$c_{ij} \;=\; (Z_i - \bar{Z})(Z_j - \bar{Z}) \tag{2}$$

and grouping them, in the case of an isotropic covariance function, in distance intervals

$$h_1 = [0, w], h_2 = (w, 2w], \ldots$$

the experimental covariance function

$$\text{cov}(h_k) \;=\; \frac{1}{N_K} \sum_{\{\mathbf{p}_i, \mathbf{p}_j\} \in h_k} (Z_i - \mu)(Z_j - \mu) \tag{3}$$

is constructed, where N_K denotes the number of pairs of observations in distance interval h_k. In a next step a positive definite theoretical covariance model is fitted on the experimental covariance function in order to obtain a continuous covariance function $C(.)$. Fulfillment of the positive definiteness condition will guarantee in a later step that the Kriging system always has an unique solution. Typical covariance models that are often used are the spherical, exponential and Gaussian models. In case of predicting the large scale component the Gaussian model

$$C_G(h) \;=\; \sigma_2 e^{-\frac{(3h)^2}{R^2}}, \tag{4}$$

is likely to give the best result, because the first derivative vanishes in the origin, which implies that the covariance initially is not dropping too quickly. In the other two models the covariance drops initially much faster, therefore more weight is given to close by observations. In Equation (4), σ^2 stands for the variance of the observations and R for the correlation range, that is, the shortest distance at which two observations can be considered to be independent. Using a Gaussian model can cause instabilities in the Kriging system and should therefore always be used in combination with at least a small nugget effect in a way that will be explained later.

2.2 The Ordinary Kriging system.

The Ordinary Kriging method determines the Best Linear Unbiased Predictor (BLUP) for a height $\hat{Z}_0 = \sum_{i=1}^{n} w_i Z_i$ from AHN observations $Z_1, \ldots, Z_n$, given a covariance function

$$\text{cov}(\mathbf{h}) : \mathbb{R}^2 \rightarrow \mathbb{R} \tag{5}$$

and an unknown mean. This height prediction $\hat{Z}_0 = \sum_{i=1}^{n} w_i Z_i$ is optimal in the sense that it minimizes the expected error variance, given the unbiasedness condition, which states that the expected error $E\{\hat{Z}_0 - Z_0\}$ between the height prediction $\hat{Z}_0$ and the real, unknown height Z_0 equals zero. It can be shown that the weights that correspond to this optimal solution are obtained by solving the ordinary Kriging system $\mathcal{C}_n \cdot \mathbf{w}_n \;=\; \mathbf{d}_n$, with

$$\mathcal{C}_n \;=\; \begin{pmatrix} C_{11} & \ldots & C_{1n} & 1 \\ \vdots & \ddots & \vdots & \vdots \\ C_{n1} & \ldots & C_{nn} & 1 \\ 1 & \ldots & 1 & 0 \end{pmatrix} \tag{6}$$

the so-called redundancy or variance-covariance matrix that contains the pair-wise covariances, in our case obtained from the fitted Gaussian covariance function:

$$C_{ij}(\mathbf{p}_i, \mathbf{p}_j) \;=\; C_G(\|\mathbf{p}_i - \mathbf{p}_j\|) \tag{7}$$

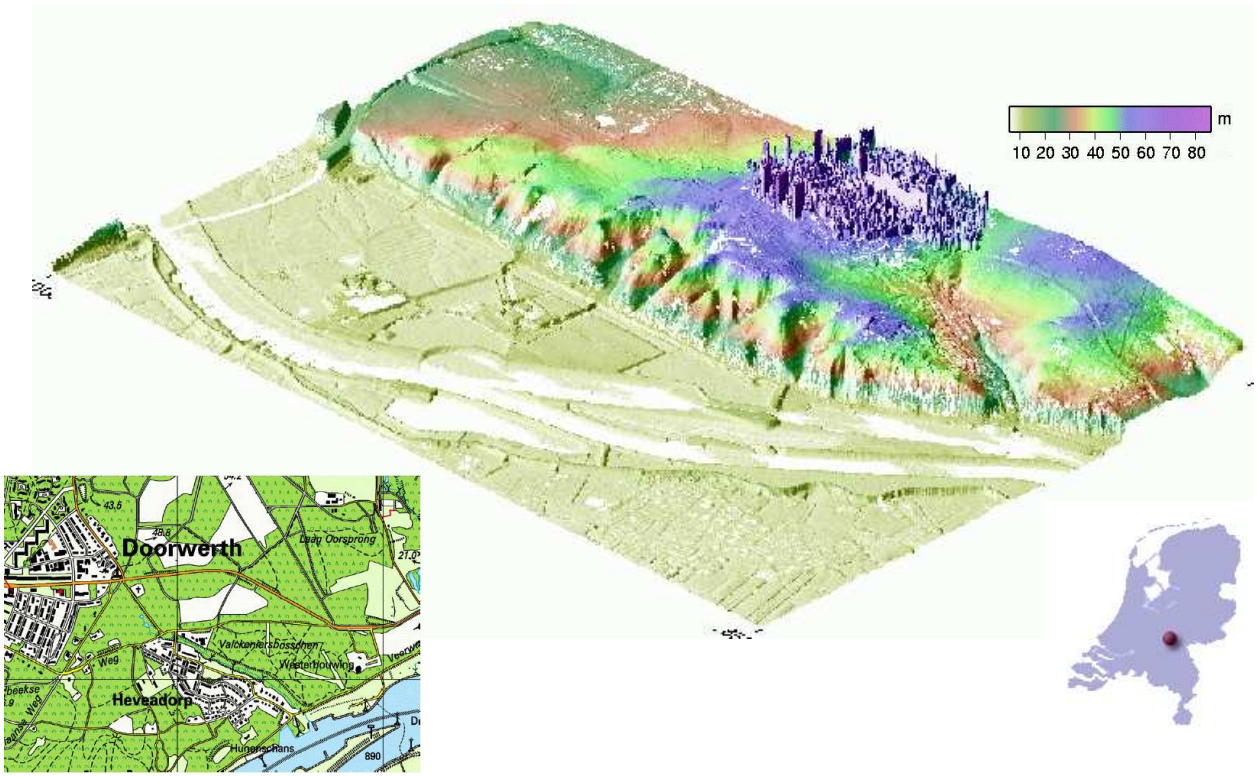

Figure 3. Large figure: topography of the Doorwerth area, with exaggerated heights in meters. The river Rhine is in the front, the village of Doorwerth is clearly visible on the plateau. The Celtic fields are situated on the plateau, on the right hand side of Doorwerth. The bottom-left figure shows an extract of a local topographic map. The first part of the Celtic field system was found in the forest on the North-East of the curved road. The new method shows that the field system continues on the South-East part of the road as well. On the bottom-right figure the location of Doorwerth in The Netherlands is indicated by the dot.

and with

$$\mathbf{d}_n \;=\; \begin{pmatrix} C_{10} \\ \vdots \\ C_{n0} \\ 1 \end{pmatrix}, \text{ and } \mathbf{w}_n \;=\; \begin{pmatrix} w_1 \\ \vdots \\ w_n \\ \lambda \end{pmatrix}, \tag{8}$$

the proximity vector and the weight vector, resp. The proximity vector, $\mathbf{d}_n$, contains the covariances

$$C_{i0} = C_G(\|\mathbf{p}_i - \mathbf{p}_0\|) \tag{9}$$

between the prediction location $\mathbf{p}_0$ and the observations. Solving the system is always possible, because of the positive definiteness of the covariance function, and the unique solution gives the weights $w_1, \ldots, w_n$ corresponding to the BLUP. To ensure that the solution found is indeed unbiased, the final row of the system contains the additional condition that the weights sum up to one. Therefore an extra variable is added to the weight vector, the Lagrange multiplier λ.

2.3 Filtering.

The Ordinary Kriging system as formulated as above is exact, which means that all the observations are respected: the BLUP at an observation location is the observation itself. This is not what we want, as we want to decompose our observations Z into a large scale component Z^M and a micro scale component Z^m, that is

$$Z_i(\mathbf{p_i}) \;=\; Z_i^M(\mathbf{p_i}) + Z_i^m(\mathbf{p_i}) \tag{10}$$

In order to obtain $Z_i^M(\mathbf{p_i})$ as a prediction, we have to filter the micro scale component $Z_i^m(\mathbf{p_i})$ out of the prediction $\hat{Z}_i(\mathbf{p_i})$. This can be achieved by modeling the micro-scale variations by a so-called nugget effect. The nugget is a general term for variations in the signal on such a short scale that it cannot be distinguished if these variations are due to measurement errors or really occur in the observed attribute. A nugget value, N, can either be determined out of the structural analysis, or by taking the specified measurement error, but can also be given an artificial value, just to obtain a required result. To filter the nugget out of the prediction, it has to be added only to the left site of the Ordinary Kriging system $\mathcal{C}_n \cdot \mathbf{w}_n = \mathbf{d}_n$, that is, the Kriging system is rewritten as:

$$\begin{pmatrix} C_{11}+N & \ldots & C_{1n} & 1 \\ \vdots & \ddots & \vdots & \vdots \\ C_{n1} & \ldots & C_{nn}+N & 1 \\ 1 & \ldots & 1 & 0 \end{pmatrix} \cdot \mathbf{w}_n = \begin{pmatrix} C_{10} \\ \vdots \\ C_{n0} \\ 1 \end{pmatrix}$$

In this way, the micro scale variations (the nugget) have no influence in the right-hand proximity vector. This implies that, when predicting at an observation location, the Kriging system is in fact told that there is no observation available at zero distance.

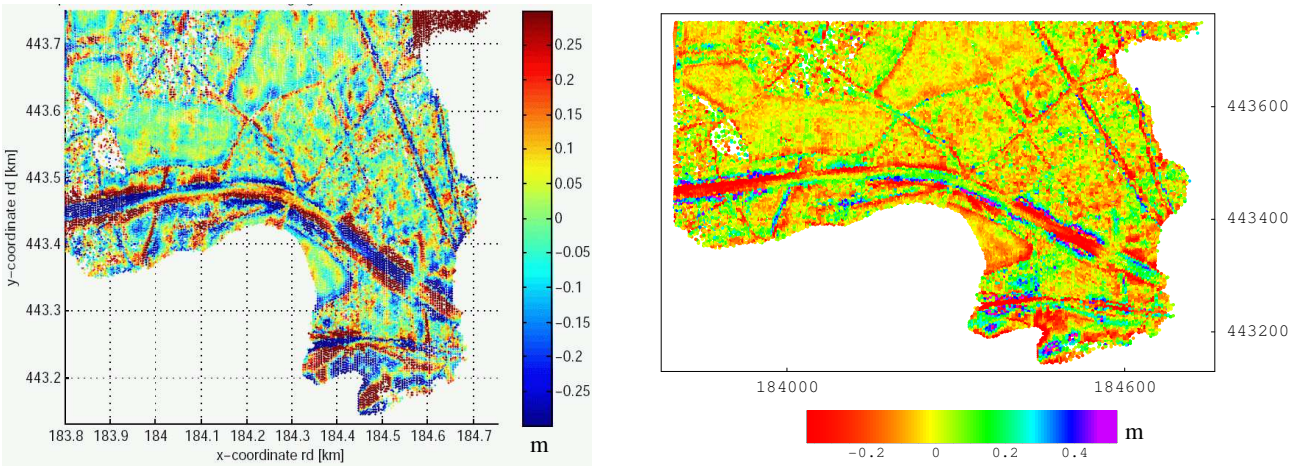

Figure 4. Two different scatterplots of the laser altimetry data residuals after filtering. The Celtic fields pop up as yellow lines on the left and as light green on the right.

Therefore the Kriging system behaves as if it is away from an observation location and gives a prediction based on the different observations, that is, it is not exact anymore. Moreover, the influence or weight attached to close-by observations is relatively low because of the extra nugget in the variance-covariance matrix that is not occurring in the proximity vector.

By determining the solution of this Kriging system at every observation location $\mathbf{p}_i$, the observation wise large scale components $Z_i^M(\mathbf{p}_i)$ are obtained, and therefore also the micro scale components. If the number of observations is not too big, say smaller than 1000, the variance-covariance matrix $\mathcal{C}_n$ only needs to be built once and can be used for every observation-wise prediction. Alternatively, local neighborhoods, consisting of the, say, 100 closest points can be used to fill observation-wise variance-covariance matrices.

3. DATA DESCRIPTION AND FILTER RESULTS

In this section first the data is introduced and some preprocessing steps are described. Then the parameters used in the filtering are discussed. Finally the results of the filtering method on the data are presented.

3.1 Data description

The full data set consisting of 1 883 056 height observations is visualized in Figure 3 in such a way that the height differences are exaggerated. In the bottom of the figure the river Rhine is clearly visible as the area where no height observations are available. Around the river, the river dikes are recognizable as well. North of the river a plateau of about 40 meter high steeply rises out of the river valley. This plateau is an ice pushed ridge resulting from the second-last ice age.

On top of the plateau, the village of Doorwerth is situated. On the East of Doorwerth the Celtic field system was revealed by illumination of the unfiltered data (after removal by the Ministry of Public Works of the tree points), compare Figure 2. Around this area a crop of the full data set was made, resulting in a reduced data set of 103 699 points. This data set was further reduced by removing all points below 45 m as these points clearly are not on the plateau. Finally, about 50 000 observations remain to be processed. A full specification of the AHN laser altimetry product can be found in the product description, (Anonymous, 2000).

3.2 Kriging parameters

First a structural analysis was performed for the reduced data set. Still, for 50 000 points it is not feasible to determine pair-wise experimental covariances for all pairs of points, therefore a random subset of 4000 points was considered. In general this practice may result in an under-sampling of point pairs on short distance. Here this is not a problem, because we are more interested in the long scale variability anyway. By determining an experimental variogram (equivalent to a covariance function in case of stationarity) a nugget value of 7.17 cm was found. In comparison, AHN specifies a Root Mean Square error of 20 cm for forest areas, (Anonymous, 2000). Fitting of a Gaussian model resulted in a value for the correlation range of 625 m. Then the smoothed Ordinary Kriging predictions were obtained for all observations in the reduced data set, using a local neighborhood of 600 points.

3.3 Filtering results

By filtering away the large scale component out of the AHN observations, the residuals as visualized in Figure 4 were obtained. The boundary on the south corresponds to the 45 m contour line of the original observations. A histogram of the residuals is given in Figure 5. The mean residual is 1.16 cm, which shows that the residuals are almost not biased. The standard deviation of the residuals is 16.7 cm. In Figure 4, the main road from left to right is the most prominent, followed by some linear features that represent smaller roads and footpaths as can be seen in the topographic map of Figure 3. In between the road and the footpaths a network of of rectangular patches is visible that is surrounded by small embankments of maybe 10 cm high. From this figures it can an also be concluded that the field system continues on the South of the road.

4. CONCLUSIONS

In this article one method is given to filter the large scale topography component out of laser altimetry observations. This method

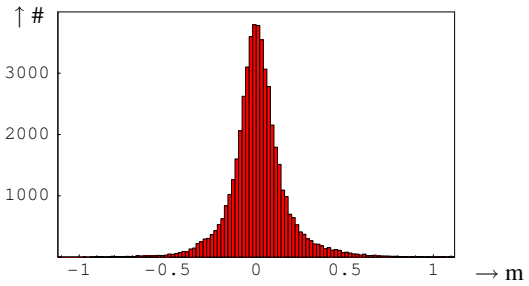

Figure 5. Histogram of the residuals after filtering.

helps to visualize micro-relief features, in this case Celtic field systems. Even in a forested area with many roads and footpaths it is in this way possible to reveal such low-elevation features.

Disadvantage of this method is that it is computationally not so fast. Either a large variance-covariance matrix needs to be converted or many local neighborhoods should be determined. There exist however other approaches, like Fourier approximation like methods that may be more time efficient.

A next step could be to enhance the visualization by removing non-relevant features, like the above-mentioned roads and footpaths. Moreover it is possible to extract line elements, like the small embankments around the fields, automatically by means of e.g. a Hough transform, (Boyle and Thomas, 1988).

ACKNOWLEDGMENTS

The authors would like to thank the Adviesdienst Geo-informatie en ICT for providing them with the AHN data.

REFERENCES

Anonymous, 2000. Productspecificatie AHN 2000. Technical report, Rijkswaterstaat, Meetkundige Dienst. http://www.ahn.nl, last visited: July 14, 2006.

Boyle, R. and Thomas, R., 1988. *Computer Vision:A First Course*. Blackwell Scientific Publications.

Chilès, J.-P. and Delfiner, P., 1999. *Geostatistics: modeling spatial uncertainty*. Wiley Series in Probability and Statistics. New York: John Wiley & Sons.

Da Devereux, B. J., Amabable, G. S., Crow, P., and Cliff, A. D., 2005. The potential of airborne LIDAR for detection of archaeological features under woodland canopies. *Antiquity* 305(79), 648–660.

De Boer, A. G., Laan, W. N. H., Waldus, W., and Van Zijverden, W. K., ToAp. Lidar-based surface height measurements: applications in archaeology. Technical report, British Archeology Reports International Series. To appear.

Goovaerts, P., 1997. *Geostatistics for Natural Resources Evaluation*. New York, Oxford: Oxford University Press.

Koch, K.-R., 1999. *Parameter Estimation and Hypothesis Testing in Linear Models*. Springer.

Lindenbergh, R., van Dijk, T., and Egberts, P., ToAp. Separating bedforms of different scales in echo sounding data. In *Proceedings 5th International Conference on Coastal Dynamics 2005*, Barcelona. To Appear.

Sithole, G. and Vosselman, G., 2004. Experimental comparison of filtering algorithms for bare-earth extraction from airborne laser scanning point clouds. *ISPRS Journal of Photogrammetry and Remote Sensing* 59(1-2), 85–101.

Spek, T., Groenman-van Waateringe, W., Kooistra, M., and Bakker, L., 2003. Formation and land-use history of Celtic fields in north-west Europe - An interdisciplinary case study at Zeijen, The Netherlands. *European Journal of Archaeology* 6(2), 141–173.

Teunissen, P. J. G., 2000. *Adjustment theory*. Delft: Delft University Press.

Wackernagel, H., 2003. *Multivariate Geostatistics* (Third ed.). Berlin: Springer.

Zijverden, W. v. and Laan, W., 2005. Landscape reconstructions and predictive modeling in archaeological research, using a LIDAR based DEM and digital boring databases. In *Archologie und Computer. Workshop 7*, Vienna, 2003.